

## Laser induced collisions between Lithium isotopes

Evgueni V. Kovarski  
*ekovars@netscape.net*  
(07.17.2001)

### Abstract

The near resonant cooling mechanism have offered for the experiment with laser induced excitation of Lithium isotopes and its ionization by collisions.

32.80.

## I. INTRODUCTION

Clearly defined spectrum is the main requirement for any spectroscopical methods, which deal with two close isotopes as  $Li_6$  and  $Li_7$ , It is preferable to use the atomic beams, where it is easy to realize the excitation of single spectral line of  $Li_6$  or  $Li_7$  [1]. However there are many publications devoted to the general study of Lithium vapor in the heat-pipe oven. There is the Doppler broadening of spectral lines. It is necessary to have a stability and accuracy frequency adjustments of the laser. Usually for Lithium atom the single mode laser operation is need with stability and tuning of the laser frequency better then 1  $GHz$  at the resonant frequency. The first known publication with Lithium resonance ionization spectroscopy (RIS) was in 1977 [2]. There were photo-ionization cross section going from the  $2P$  level and the demonstration of the ion current by varying the dye laser wavelength correspondent to  $2S - 2P$  transition. Therefore this was the first work about the possibility of Lithium laser isotope separation. Two years later the US patent for Lithium laser isotope separation was accepted in 1979 [3]. The resonance ionization spectroscopy (RIS) of Lithium use two lasers with different frequencies. It is depend on intensities of both lasers for resonance excitation at  $2S - 2P$  and for the ionization from  $2P$  [4] (1982). The mixture of two gases in heat pipe usually is present due to chemical activity of Lithium contacts with optical windows of the heat-pipe oven. The Ar gas usually is present. Therefore one can to compare ions production by RIS in the heat-pipe with another similar method for the  $Li - Ar$  contact ionization based on the ion cyclotron resonance (ICR) isotope separation [5]. It should be noted here that we shall not discuss the effectiveness methods of isotope separation, but on the other hand, both RIS and ICR can work more successfully at experiments where the concentration of Lithium atoms is high. To achieve high values of concentration it is necessary to increase the temperature of  $Li$  of a vapor chamber with the metallic Lithium. The ion generation process is important for some applications at similar condition of environment. We consider collisions at the experiment with heat-pipe oven, filled with  $Li - Ar$  mixture For such experiment the electromagnetic properties of gas mixture play an important role due to relatively high concentration of charged particles produced by emission, atomic collisions and proper RIS for ionization. The geometric distribution of generated positive and negative particles in the gas chamber is along the way of coaxial laser beams. If there is no voltage applied to electrodes the small value of electric current is only due to atom - field interaction. Because the heat pipe oven has two electrodes with cylindrical symmetry and proper laser is as new cylindrical electrode that produced charged particles along the laser way.

We are going to present: the simplified method for spectroscopic investigation of the dense vapor of  $Li - Ar$  mixture, based on methods of atomic collision estimations; the experimental setup for ionization experiment with lasers, precisely tuned on transition frequency; the results of electric current measurements. The ion generation is with both the RIS and without it. Last process is most interesting to that the ultra-violet radiation is absent and for achievement of a threshold of ionization is no sufficiently only to excite  $2S - 2P$  transition. In both cases the quantity of the charged particles can appear so large, that it is possible to speak about presence low density plasma [6]. The measurement of the excitation and ionization of dense lithium vapor by cw- dye laser with wavelength 610.3nm were performed in Ref. [7]. In present work the result was obtained by using only 670.8nm wavelength. When the DYE laser excite  $2P$ -level at 1,848 eV it can not reach to  $3D$  energy

level at 3,879 eV due to 2,031 eV difference for two steps excitation and it can lower the ionization potential at 5,391 eV of *Li* atoms. For this reason we think that there is not a special two-step absorption process, so we will to discuss two mechanisms such as associative reaction and near resonance cooling.

## II. SPECTRAL CHARACTERISTICS OF THE DENSE LITHIUM VAPOR.

We begin with note that the main problem for such experiments is about the relative values for concentrations of neutral atoms and molecules in the same *Li* vapor. Of course, special measurements for molecules or clusters concentration are needed on time (for *Li* molecules studies see e.g. ref [8]). The standard experimental absorption intensity spectrum of the  $2S - 2P$  of each Lithium isotopes has two spectral lines *D1* and *D2* [1] with correspondence to level isotope shifts [9]. The Lithium  $2S - 2P$  has one doublet with distance of 10 GHz (0,012 nm) between *D1* and *D2* spectral lines. The isotope shift between *Li<sub>6</sub>D2* (670,7922 nm) and *Li<sub>7</sub>D2* (670,7764 nm) is 10,5333 GHz and between *Li<sub>6</sub>D1* (670,8073 nm) and *Li<sub>7</sub>D1* (670,7915 nm) is 10,5329 GHz [1].

Usually the observable at heat-pipe experiment  $2S - 2P$  spectrum of natural Lithium consists of three lines, where the central line is formed by the superposition of two lines going from two different isotopes [3]. At heat-pipe experiments with the dense *Li* vapor at high temperature, above 1000 K, all Gauss lines profiles can not been clearly observed. There are only three observable normalized profiles of absorption intensity received from experiment and fitted numerically. The well known picture of the fine structure for each isotope was not at high temperature heat pipe experiment, but particularly was revised with two diode laser for calibration.

The Voigt profile approach can be applied for simple analysis of the Doppler broadened line and for the Lorentzian line, which widths are related to the correspondent Gauss to Lorentz ( $G/L$ ) damping constant. With known value of the ( $G/L$ ) damping constant from fitted profile, it is easy to obtain the line width for Lorentzian profile and evaluate the summary of excitation transfer mechanisms. Also special experiments and theory are needed for detailed investigation of *Li* atoms collisions [10] - [13].

We use the method based on dense gas absorption intensity spectrum [Fig. 2] that can be analytically described by empirical approximation for a Voigt profile of the absorbed intensity in the Beer law, where the absorption coefficient  $k_{abs}$  is [14]:

$$k_{abs} = k_G \left[ e^\eta - \frac{2a}{\sqrt{\pi}} (1 - 2\eta F) \right], \quad (1)$$

The absorption coefficient for Gauss line profiles is  $k_G$ . The coefficient  $k_G$  can be founded numerically from fitted profiles of absorption intensity, because the application of the Beer law with absorption coefficient as a constant, which no depend on Gauss distribution is not correct for a dense vapor. Also at a maximum of one unsaturated line is possible to compare  $k_G$  form fitted spectrum with the same value from the Beer law, therefore is possible to use the thickness (8,5 cm) of dense vapor. There are two numerical parameters for normalized profile of intensity  $I_{abs}/I_0$ , where  $I_0$  is the intensity of the laser. One of these parameters is  $k_G$ , which depend on spectral lines saturation, e.g. for *Li<sub>6</sub>* and *Li<sub>7</sub>* due to accordingly

concentrations. The  $\eta$  is the second numerical parameter. It dependent on wings of spectral line at frequency  $\nu$ , which are far from the central line  $\nu_0$  for both isotopes:

$$\eta = \frac{(\nu - \nu_0)}{\Delta\nu_G} \sqrt{\ln 2}, \quad (2)$$

For unsaturated spectral lines, as for left spectral profile in the [ Fig. 1 ], that corresponds to  $Li_6$ , the parameter  $\eta$  leads to the function  $F$  for the Voight profile:

$$-2\eta F = 1 - 2\eta^2 + \frac{4}{3}\eta^2 - \frac{8}{15}\eta^6 + .. \quad (3)$$

and the  $(G/L) = a$  damping constant is

$$a = \frac{\Delta\nu_L}{\Delta\nu_G} \sqrt{\ln 2}. \quad (4)$$

The Eq. (3) is used only for the fitting  $Li_6$  spectral lines, because the parameter  $\eta$  for  $Li_6$  is not too large as for  $Li_7$ , due to the relative concentrations of these isotopes. For  $Li_7$  isotope spectral line the saturation is much more greater than for  $Li_6$ , thus in this case the Voight profile must be fitted by using the other sequence:

$$1 - 2\eta F = - \left( \frac{1}{2\eta^2} + \frac{3}{4\eta^2} + \frac{15}{8\eta^6} + \dots \right) \quad (5)$$

By fitting the experimental spectrum with above method is possible to obtain a better result with experiment for each spectral line. Also another empirical approximation of Voight profile [15] can be used successfully for all spectral lines at the narrow part of frequency spectrum.

The  $(G/L)$  damping constants for both  $Li_6_{D1}$  and  $Li_7_{D2}$  have the same values  $a_7 = a_6 = 0.021 \pm 0.0005$  and both absorption coefficients for  $Li_7$  and  $Li_6$  were estimated from fitted spectrum at a fixed temperature.

The relation of two Gaussian profiles for  $Li_7$  and  $Li_6$  at fixed temperature is:

$$\frac{\Delta\nu_{G6}}{\Delta\nu_{G7}} = \frac{\nu_{6D1}}{\nu_{7D2}} \sqrt{\frac{\mu_7}{\mu_6}} = 1,08, \quad (6)$$

where  $\mu_6 = 6,01703a.u.$ ,  $\mu_7 = 7,01823a.u.$  and resonance frequencies corresponds to wavelength 670,7764 nm for  $Li_7$  and 670,8073 nm for  $Li_6$ . At temperature  $T = 831.84K$  and pressure 1.8torr, the full width of the half maximum (FWHM) is  $\Delta\nu_{G6} = 3763.17MHz$  for  $Li_6_{D1}$  and  $\Delta\nu_{G7} = 3484.58MHz$  for  $Li_7_{D2}$ .

For correspondent Lorentzian profiles one can easy to calculate the FWHM equal to  $\Delta\nu_{Li6} = 94.92MHz$  for  $Li_6_{D1}$  and  $\Delta\nu_{Li7} = 87.89MHz$  for  $Li_7_{D2}$ .

The heat velocity of atoms in the  $Li - Ar$  mixture is:

$$\bar{v} = \sqrt{\frac{8k_B T}{\pi M}} \quad (7)$$

Also the numerical equation for corresponded temperature dependence is  $\bar{v} = 63.64\sqrt{T}$ , where the reduction mass is  $M = (M_{Li}M_{Ar}/M_{Li} + M_{Ar}) = 0.8683 \cdot 10^{-26}kg$ .

Therefore, with the temperature about  $650\text{ K}$ , the random velocity of the  $Li - Ar$  atoms vapor is about  $160\ 000\text{ cm/s}$  and the correspondent Doppler shift for one laser wave is about  $16\text{ GHz}$ . There are some experimental possibilities for measurements. When the laser has frequency scanning along spectrum of Lithium, the relative datum can be used for the line position in the spectrum due to the Doppler shift for each wavelengths. The Doppler-free method, that used two opposite propagated beams with the same frequency on the each laser beam is free of the Doppler shift for detectors, thus the Lorentzian profile can be experimentally received, but only calibrated relative scale of the frequency can be used for estimation of the Lorentzian profile. Therefore the  $20\text{ GHz}$  scale between known spectral lines captured from the literature datum for  $Li$  is no good for Doppler-free experimental estimations of the Lorentzian profile in the gas chamber, because expected value of the FWHM is about  $100\text{ MHz}$  and special calibration laser air wavelength is needed. Also if the one of two laser beams is controlled by wave meter and another laser is controlled by a power meter or by photo diode with oscilloscope, thus the resolution of the wave meter is about  $0,0002\text{ nm}$  or  $133\text{ MHz}$  at  $670\text{ nm}$  and can not permit well accuracy for experiments with a Heat-pipe oven where all spectral lines are Doppler broadened and saturated. The  $2S - 2P$  transition of Lithium isotopes is well known for the all 4 principal spectral lines including the fine structures ( $fs$ ). Each atom has the lowest  $2S$  level with two ( $fs$ ) levels, which can be observed only at the special experiment with electric or magnetic fields. The distance between both  $fs$  levels is  $803\text{ MHz}$  for  $2S$  and  $18\text{ MHz}$  for  $2P$  level. Yet, we can put fine structures ( $fs$ ) out of our consideration the resonance  $2S - 2P$  transition with resonance frequency  $\omega_0 = 2,8 \cdot 10^{15}\text{ rad./s.}$ , because the Doppler - free method can not to permit the accuracy experiment with a given transition.

### III. EXPERIMENTAL SETUP

The selection and specification of special designed lasers instrumentation for selective excitation of lithium isotopes and full ionization is important because of the small frequency distance between the lithium lines is present and it is necessary to study some laser spectral stability characteristics. The experimental setup [ Fig. 2] consists of three lasers which path is the same route across the heat-pipe oven. This is possible by use properties of Glan prisms and rotators of polarization.

The lasers wavelength was controlled by a serial pulsed Burleigh wave meter Model WA 4500 with accuracy  $0,0001 - 0,0002\text{ nm}$  at wavelength range from  $1100\text{ nm}$  to  $400\text{ nm}$ . The laser line shape was measured by use of a Burleigh Spectrum Analyzer System SA 385 with SA-91 Etalon Assembly. Its maximum specified resolution is  $27\text{ MHz}$  using  $8\text{ GHz}$  FSR mirror set with finesse about 300 and the transmission more then 10 as a Fabry-Perot filter with thermal sensitivity  $70\text{ nm}/^\circ\text{C}$  changing in mirrors spacing.

The laser power was measured with a cw - Laser Power Meter, Spectra Physics, Mod 407 A. It has a wavelength range  $250 - 1100\text{ nm}$ , power range from  $5\text{ mW}$  to  $20\text{ W}$  with sensitivity variation about 1 because the damage peak energy density is  $0,3\text{ J/cm}^2$  at  $50\text{ ns}$  pulses. Also the 818 UV, Newport Power Meter was used for precisely measured power of low intensity cw - lasers.

For the ionization process we used a High Power  $Q$ -Switched,  $TEM_{00}$  frequency-doubled Nd-YAG *Lee* Laser, Model  $815TQ$ . The power stability was  $10\ 1064\text{ nm}$  was  $15\text{ W}$  at 5

*kHz* repetition rate (pulse energy 2,2 *mJ* and pulse duration 90 *ns*) and the intensity 3 *MW/cm<sup>2</sup>*. In this configuration the second harmonic wavelength (532 *nm*) is emitted laterally from the optical axis of the laser resonator. The SHG assembly contains a KTP (potassium titanyl phosphate crystal) which is bounced inside a temperature controlled chamber. Because of the small crystal cross section (4 x 4 *mm*), there is a little box for misalignment of the crystal with the Nd-YAG beam optical center line. The average power was 2,5 *W*, the average energy was 0,5 *mJ* and the pulse duration was 100 *ns*. We worked with 1,5 *W* for obtaining UV 266 *nm*. For this purpose we used an INRAD temperature stabilized crystal of *KDP*, obtaining 40 *mW* of the average power. The non-critical phase matching temperature (35 °C - 75 °C) is quite dependent on the deuteration level of the *KDP*. Also the incoming edge of the crystal is at 90 ° with the optical axis of the crystal and the reflection at the angle about 23 ° decrease the intensity of 532 *nm* about two times. The lineal polarization of 532 *nm* going from the *LEE* laser had an inclination with the angle 45 ° respect to the optical path of our experiment. The specially oriented crystal *KDP* for second harmonic generation (*SHG*) was needed. From two waves within one laser beam with  $\lambda = 532 \text{ nm}$  the well known procedure of the second harmonic generation was used. The wave with  $\lambda = 266 \text{ nm}$  We obtained a UV-beam at 266 *nm* with intensity 16 *kW/cm<sup>2</sup>* after the prism separation from incoming 532 *nm* wave. The line width of the UV line was 20 *MHz* with high frequency stability. Frequency stability of the ionization laser is no so critical as for the excitation process, because for ionization we have a transition from *2P* to above ionization limit.

The group of calibration lasers consist both the 6202 *NewFocus* diode laser and the *EOSI* diode laser with line width about 100 *KHz* and the average power 6 *mW*. These lasers was used for calibrating the experiment due to high stability parameters at the needed wave length.

We tested a cw - broadband standing-wave Spectra Physics DYE Laser (Model 375 B), because we can change the mode structure of outgoing laser wave as a special background for given laser equipment [16]. The DYE laser was pumped by a power  $P_0 = 6W$ , Stability Multiline Ar-Ion Laser Spectra Physics Model 2017 -06 S. The Ar-ion laser had some measurable spectral lines, such as: at 514,5 *nm* with 0,393  $P_0$ , at 496,5*nm* with 0,166  $P_0$ , at 488 *nm* with 0,285  $P_0$ , at 476,5*nm* with 0,109  $P_0$ , at 457,9 *nm* with 0,047 $P_0$ . The amplitude stability of the DYE laser intensity was best with pumping of the Ar-Ion laser at 514,5 *nm*. The DYE laser was based on DCM 4 -(Dicyanomethylene) - 2 -(methyl) - 6 -(*p* - dimethylaminostyryl)- 4-*H*-(pyran) with molecular weight 303,37 *a.u.* and concentration 1,5 (*mmole/l*), which was prepared when 0,682*g* of the DCM was solved in Propylene carbonate (0,6 *l*) and Ethylene Glycol (0,9 *l*). The absorption curve of DCM has an absorbency region between 450 *nm* and 550 *nm*. The broad band emission curve has the FWHM about 80 *nm* at 650 *nm*, which is close to the resonance *2S* – *2P* transition of Lithium at 671 *nm*. The Spectra Physics data for the Model 375 B laser were: power 600 *mW* at 705 *nm*, line width 7 *GHz*, amplitude stability less then 0,5 accuracy of wavelength changing 0,5 *nm*. The limit of wavelength changing is in the same order as a Rayleigh selection rule for spectral lines  $8/\pi^2$ , that is about 0,5 *nm* for a given laser line width. We obtained characteristics of Spectra Physics DYE laser, Model 375 B, such as: average power 1,2 *W* at 671 *nm*, accuracy of changing wavelength better then 0,01 *nm* and frequency stability about 0,0001 *nm/hour* during time of the experiment. All parame-

ters are depended on needed laser modes structure and corresponds to properties of optical elements inside the resonator. For our experiments with  $Li$  we modified the mode structure and the spectral line width of outgoing laser wave by inserting an additional etalon into a laser resonator. We note that broadband laser had the tuning accuracy  $0,5 \text{ nm}$  without  $E1$  due to  $BF$  frequency tuning accuracy. With  $BF$  and  $E1$  the frequency tuning accuracy was measured  $\approx 0,0001 \text{ nm}$ . The first air spaced etalon ( $E1$ ) had a temperature stability. When the  $BF$  and  $E1$  were used, the output frequency of the DYE laser was tuned to the quite frequency  $4,46789597 \cdot 10^{14} \text{ Hz}$  by used the angle and temperature tuning of  $E1$ . The FSR of output frequency was  $19,655 \text{ GHz}$ . Then the second etalon  $E2$ , with  $\text{FSR} = 15 \text{ GHz}$  was installed inside the cavity and the same operation was repeated with angle tuning of  $E2$  for the same frequency. The  $E2$  was chosen, because the spectral lines of the Lithium have  $10 \text{ GHz}$  distance twice between 3 spectral lines and laser with  $BF$  and  $E1$  can excite both  $Li_6$  and  $Li_7$ . The single mode operation of the broad band laser was achieved. The single mode selection was realized experimentally [Fig. 2] by use the aperture with diameter  $1 \text{ mm}$  for transverse mode selection and, by use two etalons ( $E1, E2$ ) and the birefringent filter ( $BF$ ) for longitudinal mode selection. The mode structure of the single laser beam is very important for selective excitation. There are some experimental possibilities with the broad band DYE laser, which depend on needed experiments. The single mode operation was necessary for a RIS experiments. On the contrary for measured values of electric current [Fig.3] of the laser induced low density plasma observation experiment [6], the DYE laser had the two longitudinal modes with FWHM  $100 \text{ MHz}$ , separated exactly at  $20 \text{ GHz}$  with cavity etalon. This etalon had the free spectral range (FSR) that correspondent the distance between two spectral lines of  $Li_6$  and  $Li_7$  isotopes of the natural Lithium vapor. The laser was tuned exactly on  $670.8073 \text{ nm}$  for  $Li_6$ . Another wavelength  $670.7716 \text{ nm}$  was not controlled. The average power at this experiment was  $100 \text{ mW}$ . There are some known methods of longitudinal mode selection by use interferometers techniques as in [17], [18]. The free spectral range FSR is equal to the distance between two longitudinal modes:

$$FSR_\nu = \frac{c}{2\eta_t d \cos \Theta_i} \quad (8)$$

Thus, with variation of the angle, some longitudinal modes of the laser will have not losses for correspondent frequencies  $\nu = m, (\text{FSR})$ , and it is possible to move the Airy spectrum of the etalon along the frequency axis up or down to quite position. The longitudinal modes are spaced in frequency by  $c/2L$ . We note that for near-confocal resonator the free spectral range (FSR) is:

$$\delta\nu = \frac{c}{4L + \frac{x}{\rho^3}}, \quad (9)$$

where  $(x)$  - is the distance from the axis and  $\rho$  is the radius of mirrors, when  $L = \rho$ . Thus the series of longitudinal modes are separated by  $c/4L \approx 250 \text{ MHz}$  for a cavity with  $L \approx 30 \text{ cm}$ . Transverse modes are important for a mode selection too. Amplitude distribution of these modes is given with Hermit polynomial  $TEM_{mn}$  modes. The separation of the first transverse mode ( $m = 0, n = 1$ ) from the axial mode is:

$$\frac{\nu_1 - \nu_0}{\nu_0} = 2,405 \frac{\lambda^2}{8\pi^2 r^2}, \quad (10)$$

where ( $r$ ) is diameter of cylindrical laser material. In deriving the Van Cittert-Zernike theorem [19] it follows that the diffraction pattern would be obtained on replacing the source (the DYE luminescence cross section) by a diffraction aperture of the same size and shape as the source. The amplitude distribution over the wave front in the aperture being proportional to the intensity distribution across the source. The calculation of the complex degree of coherence of light from an incoherent source, by use the Hopkins formula [19], leads to the mirrors diameter  $0,32 \lambda f/h$ , where ( $f$ )- is focal distances ,  $h \approx 10 \mu m$  - is the diameter of the source, that dependent on a pumping of the focused laser (6 W Ar-Ion laser) and thermal lens. At flow velocities of the DYE about 10 m/s the time of flight for the dye molecules through the focus is about 1  $\mu s$ . By using a mirror whose reflectivity can be varied over its surface, it is possible to have some given combination of transverse modes, if it is necessary.

There are two problems of frequency stability of the DYE laser. Firstly, we note that the material of installed cavity DYE laser etalon was fused silica. Regardless of thickness it has a drift of airspace between fused silica plates about 5 GHz/ $^{\circ}C$  and would have to be temperature stable about 0,1  $^{\circ}C/hour$ . Secondly, the environment conditions are very important for stable laser experiment with atomic spectral lines. Therefore, there is the frequency drift:

$$\frac{\Delta\nu}{\nu} = \frac{\Delta d}{d} + \frac{\Delta n}{n} \quad (11)$$

where ( $d$ ) is the cavity length and ( $n$ ) is the refraction coefficient. For the quartz rod resonator structure of the DYE laser, *Model375D*, we have with respect to the change of a cavity length a resulting temperature sensitivity about 90 MHz/ $^{\circ}C$ . With respect to the refraction coefficient of air we found a temperature sensitivity about 410 MHz/ $^{\circ}C$ . The amplitude and frequency stability of the laser was maintained during 3 hours of the experiment. The wavelength control had the accuracy 0.0001 nm by use the serial wave meter. The measured value of the line width was about 100 MHz for cw -regime of DYE excitation by use the focused Ar - Ion laser. Another excitation of the same DYE laser was with 120 ns pulses of twice doubled Nd:YAG laser at 266 nm, with 5 KHz pulse repetition and average power about 1 W. Output pulses from the DYE laser were 100 ns.

#### IV. EXPERIMENTAL RESULT

For a known value of the ( $G/L$ ) damping constant and absorption coefficient from described method of the fitting we can exam the concentration of the both isotopes:

$$N_{6G} = k_{6G} \left[ \frac{2\sqrt{\pi}}{\lambda_{6D1}^2} \right] \frac{1}{a}, \quad (12)$$

$$N_{7G} = k_{7G} \left[ \frac{\sqrt{\pi}}{\lambda_{7D2}^2} \right] \frac{1}{a}, \quad (13)$$

where the absorption coefficients given from fitted profiles are  $k = 0.6 cm^{-1}$  for  $Li_6$  and  $k = 14.75 cm^{-1}$  for  $Li_7$ . The correspondent concentration going from above formulas is



equal to  $2.25 \cdot 10^{10} \text{ cm}^{-3}$  for  $Li_6$  and  $27.65 \cdot 10^{10} \text{ cm}^{-3}$  for  $Li_7$ . So the relation of two concentrations is  $N_6/N_7 = 0.08135$ , which is in well agreement with the characteristics of natural Lithium [20].

On the other hand, one can to verify values of Lithium concentration by use the following well known formula for the Lithium vapor pressure (in *torr*) at fixed temperature (in *K*):

$$P = 10^{5,055 - \frac{8023}{T}}, \quad (14)$$

where the vapor pressure for given temperature is equal to  $0.003427 \text{ Pa} = 0.0000257 \text{ torr}$ . By using the equation of the state for ideal gas  $P = Nk_B T$  and Eq.(10), one can obtain the concentration of the natural Lithium, which is equal to  $29.85 \cdot 10^{10} \text{ cm}^{-3}$ . The Heat-pipe was filled with *Ar* gas with the concentration  $10^{17} \text{ cm}^{-3}$ .

When resonance excitation of the considered system  $Li(2^2S) - (2^2P)$  was realized by  $671 \text{ nm}$  cw-laser, the ionization process was registered. The result of ionization by  $671 \text{ nm}$  was compared with additional UV laser for ionization from  $2S - 2P$  energy level ( $1,848 \text{ eV}$ ) to energy level of ionization limit ( $5,391 \text{ eV}$ ).

Intensity values of both the cw-DYE laser and the pulsed UV laser were changed correspondingly to the beam diameter  $3 \text{ mm}$  across the heat-pipe oven. We did not worked with specially applied to the heat-pipe electrodes voltage or load resistors.

Direct measurements of the electric current were performed by amper meter; maximum average value of the electric current was registered about  $30 \mu A$  [ Fig. 3 ]. We denoted three curves, where three principal effects were registered such as: (a) is the upper dependence for the RIS by use excitation and ionization from two lasers  $671 \text{ nm}$  and  $266 \text{ nm}$ . The RIS is more effective between  $450^\circ C$  and  $650^\circ C$ . (b) is the ionization current due to only  $2S-2P$  excitation with  $671 \text{ nm}$ . This specific ionization is more effective for highest temperatures. (c) is the lowest dependence (the noise) for a emission. Only small difference between average value of electric current due to the RIS process [ Fig. 3 -(a) ] and to resonance excitation  $2S - 2P$  [ Fig. 3 -(b) ]. The noise or the emission in temperature range from  $450^\circ C$  up to  $700^\circ C$  with electric current up to  $3 \mu A$  and capacitance up to  $20 \text{ nF}$  with observable saturation [ Fig. 3 -(c) ]. Values of the electric current varies from  $5 \mu A$  up to  $30 \mu A$  [ Fig. 3 -(a) ], and capacitance from  $10 \text{ nF}$  up to  $100 \text{ nF}$ . Also the capacitance of cylindrical heat-pipe was measured. The results of the current and capacitance measurements at the temperature higher than  $650^\circ C$  are the same for both mechanisms. Also it is easy to separate RIS from another ionization using the modulation signal measurements because RIS use the pulse UV laser.

## V. SOME MECHANISMS OF COLLISIONS

If the colliding particles have no charge, the trajectory  $r(t)$  is assumed to be rectilinear:  $r(t) = \rho + vt$ , where  $\rho$  and  $v$  are the impact parameter and relative velocity. The elastic collisions change the phase of damped oscillator,  $\phi(t)$ , but not the amplitude,  $x(t)$ , due to the frequency shift  $\Delta\omega$  during the phase-perturbing collisions. If the duration of collision,  $\tau_c$ , is short compared with the mean time between two consecutive collisions, one can neglect the radiation during collisions and consider the collisions to be instantaneous. Therefore the collisions are manifested only in phase shifts (Impact broadening approximation), where the

dimension parameter  $h = \rho^3 N_{Ar} \ll 1$  determines the number of perturbers in the Weisskopf sphere with the radius  $\rho$ , where the binary approximation holds. Depending on the type and states of interacting atoms both attraction and repulsion can take place at long distances. At short distances the potential is repulsive. In general case the interaction force is depends not only on spatial but also on angular variables. The results of calculations in which a more realistic interaction  $r^{-6}$  is used can not be described by a simple Lorentzian distribution, that depends on the type of the transition. The repulsive part of the interaction is usually taken into account in the form of Lennard-Jones potential. In general case, when the mean distance between the atoms is of the same order with the magnitude of atomic dimensions, simple expression for potential  $V(r) = C_6/r^6$  is valid with approximations due to both instantaneous dipole-dipole interaction and dipole-quadruple interaction with  $C_8/r^8$ .

The shift,  $\Delta\omega = 2\pi\Delta\nu$ , and broadening,  $\Gamma$ , of the Lorentz spectral distribution [21] are:

$$\Delta\nu = 2.91C_6^{\frac{2}{5}}v^{\frac{3}{5}}N_{Ar} , \quad (15)$$

$$\Gamma = 2\pi\Delta\nu_L = 8.16C_6^{\frac{2}{5}}v^{\frac{3}{5}}N_{Ar} , \quad (16)$$

For a temperature  $T = 831K$ , which we used for a fitting procedure, one can easily obtain the value for a FWHM of the Lorentzian profile,  $\Gamma = 617rad \cdot s^{-1}$  or  $\Delta\nu = 98.2MHz$  by using the coefficient in the length form  $C_6=1406$  a.u. [22] for  $Li(2^2S) - (2^2P)$ , where two interacted atoms, one of which  $2^2P$ , are in different angular momentum states with associated magnetic quantum numbers  $M_2 = \pm 1$  and attractive or repulsive interaction are. Also for  $Li(2^2S) - Li(2^2S)$  the value of  $C_6=1390$  a.u. =  $1390 e^2a_0^2 = 1.330786 \cdot 10^{-76}Cl \cdot V \cdot m^6$  [23] is closely to estimation of  $C_6$  for  $Li(2^2S) - (2^2P)$  interaction. For this reason the measured ionization gives the answer about the nature of interaction in favor of  $Li(2^2S) - (2^2P)$ .

Therefore the value of  $\Delta\nu = 98.2MHz$  which can be obtained by use  $C_6$  coefficient well corresponded to experimental results  $\Delta\nu_{L6} = 94.92MHz$  for  $Li_6 D_1$  and  $\Delta\nu_{L7} = 87.89MHz$  for  $Li_7 D_2$  from the fitting procedure.

The shift of the spectral maximum position measured at two temperature points are  $0.0126MHz/K$  or  $1.26MHz/torr$ . The value of the FWHM temperature deviation is  $0.0353MHz/K$  due to the principal temperature dependence  $\Delta\nu \simeq T^{0,3}$ , which implies the correspondent pressure changing as  $3.53MHz/torr$  (for a comparison see results for  $Li$  in ref. [24]).

The impact parameter or Weisskopf radius is [21]:

$$\rho = \left( \frac{3\pi C_6}{8 v} \right)^{0,2} \quad (17)$$

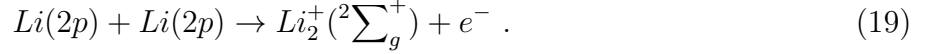
For a temperature range from  $500^\circ C$  to  $750^\circ C$  the impact parameter varies from  $6.685\text{\AA} = 12.63a_0$  to  $6.5\text{\AA} = 12.28a_0$ . The cross section is  $\sigma \simeq \pi\rho^2 = 132.7\text{\AA}^2 = 1.33 \cdot 10^{-14}cm^2$ .

The minimum concentration of charged particles in  $Li - Ar$  mixture at temperature  $1000 K$  can be estimated by taking into account the value of total current between two electrodes of Heat pipe as  $n_e \approx 10^6 cm^{-3}$ . Well-known Saha equation for amount of ionization  $n_e/n$  to be expected in a gas in thermal equilibrium

$$\frac{n_e}{n} \approx 2.4 \times 10^{15} \frac{T^{3/2}}{n_e} e^{-U_i/kT} \quad (18)$$

gives the ionization degree  $\approx 10^{-10}$  for *Li* (which concentration is  $n_{Li} \approx 10^{13} \text{ cm}^{-3}$  and ionization energy  $U_i = 5.4 \text{ eV}$ ) and  $10^{-36}$  for *Ar*, ( $n_{Ar} \approx 10^{17} \text{ cm}^{-3}$ ,  $U_i = 15 \text{ eV}$ ). So, the inelastic collisions between unexcited *Ar* and *Li* atoms could not provide the observed concentration of charge particles.

Such value of electron gas density, when DYE laser is applied [ Fig. 3 -(b) ], can be achieved due to the yield of the associative ionization reaction:



Such a process would be possible if the excited lithium atoms approached each other with relative kinetic energy about of  $0.46 \text{ eV}$  [25].

The simple approximation (18) shows that above associative ionization reaction can provide the electron densities up to  $n_e \approx 10^8 \text{ cm}^{-3}$  without the action of UV laser [ Fig. 3 -(b) ]. As for the rather high current observed even in the case when both lasers (DYE and UV) are shut down [Fig. 3 - (c)], such value of electron gas density can be achieved due to the effects of emission, mainly from the internal hot electrode with a mesh plating by Lithium.

The space-charge average current in Heat-pipe can be estimated by using the Child equation [26], due to the presence of cylindrical symmetry:

$$-I = \frac{8\pi\epsilon}{9} \sqrt{\frac{2e}{m_e}} \frac{V^{3/2}}{a\beta^2} , \quad (20)$$

where the parameter ( $\beta$ ) was determined in the Ref. [26] and ( $a$ ) is the radius of the external cylinder. The mean values for current and dielectric constant can be taken directly from current and capacitance measurements.

Given the natural line width equal to  $5,8 \text{ MHz}$  for the  $2P$  - energy level we obtain the absorption cross section

$$\sigma_{2s-2p} = 0,054 A_{2p-2s} \frac{\lambda^2}{\Delta\nu_D} \quad (21)$$

where  $A_{2p-2s} = 1/t_s$ , with  $t_s = 27,1 \text{ ns}$ . The Doppler line width of the *Li* was  $\Delta\nu_D = 2,5 \text{ GHz}$ . The absorption coefficient was  $0,154 \text{ cm}^{-1}$  in our Heat-Pipe experiment. For a given  $2S - 2P$  resonance excitation we measured absorption cross section

$$\sigma_a = 1,4 \cdot 10^{-12} \text{ cm}^2 \quad (22)$$

and ionization cross section for 266 nm ionizer:

$$\sigma_i = 1,2 \cdot 10^{-17} \text{ cm}^2 \quad (23)$$

The cathode emission current and the current of positively charged ions were also discussed in the Ref. [27].

The one-dimensional systems of driven charges can change symmetry in the phase pulses space, when the classical phenomena in one direction take into account quantization in others. It results in thermal drag effects in solids wires [28], but can result in thermal optical experiments too. Another effect is light-induced diffusive pulling (pushing) of lithium atoms into a laser beam, which was studied in Ar noble gas, where the value of diffusion coefficient  $4.3\text{cm}^2/\text{s}$  was measured [29].

It should be noted here, that the peak concentration of charged particles produced by the RIS [ Fig. 3 -(a) ] using  $77\text{ ns}$  UV pulses is much more higher than the measured average value.

An estimation, given even for the minimum value of  $n_e \approx 10^6\text{cm}^{-3}$ , gives the value of Debye length  $\lambda_D \sim 0.1\text{cm}$ , the number of charged particles inside the Debye sphere  $N_d \sim 10^5$  and  $\omega_p\nu_{ei} \sim 10^4$ , where  $\omega_p$  is the plasma frequency and  $\nu_{ei}$  is the collisions rate. It means that the *Li - Ar* mixture at temperature in the order of  $10^3\text{K}$  behaves like a plasma rather than a neutral gas [6].

By other hand we can discuss another mechanism for observed ionization . We will take the Doppler cooling as the one step to achieve the low temperature for the Bose-Einstein Condensate (BEC) at very low temperature. The limit of the temperature achieved for Lithium is  $140\ \mu\text{K}$  by balance with a scattering force in a random direction [30]. The Doppler limit of achievable temperature ( $T$ ) is:

$$k_B \cdot T = \frac{\hbar\Gamma}{2} \quad (24)$$

where  $\Gamma$  is a damping constant.

Let's change this relation:

$$k_B T = \hbar \cdot \frac{R}{R_0} = \hbar \cdot R_1 \quad (25)$$

where the rate of the power absorption  $R_1$  for two level atomic system interacted with EM field is well known:

$$R_1 = \frac{2\Omega^2\Gamma}{\Delta\omega^2 + 4\Omega^2 + \Gamma^2} \quad (26)$$

The Rabi frequency  $\Omega_\nu$  measured in ( $\text{MHz}$ ) is:

$$\Omega_\nu = \frac{d_{1,2} \cdot E_0}{\hbar} \quad (27)$$

with  $d_{1,2}$  - as the matrix dipole momentum and  $E$  as the amplitude of EM wave. There is the frequency  $\Omega$ , that make a round oscillations between two levels. When  $\Delta\omega \neq 0$  , one can used for a given *Li* atom the fixed value of the Rabi frequency  $1000\ \text{MHz.rad.}$ . Some inequalities are for given values in the denominator of the profile. One of this inequalities is evidently for an application, because the value of the Rabi frequency  $\Omega = \Omega_c = 1000\ \text{MHz.rad.}$  and  $\Gamma = 37\ \text{MHz.rad.}$  with  $\Omega \gg \Gamma$  :

$$R_1 = \pi\Omega_c\Gamma \left[ \frac{1}{2\pi} \frac{4\Omega_c}{(\omega - \omega_0)^2 + (2\Omega_c)^2} \right] \quad (28)$$

The rate  $R_1$  can be represented by use the parameter  $\rho$  that depend on the Rabi frequency and the frequency tuning value:

$$\rho = \frac{\Omega}{\Delta\omega} = \text{const} \left[ \frac{\sqrt{I}}{\Delta\omega} \right] \quad (29)$$

$$R_1 = \frac{\Gamma}{2} \left[ \frac{(2\rho)^2}{1 + (2\rho)^2} \right] \quad (30)$$

The well known saturation effect by intensity of the laser is clearly observed. Is possible to fix at experiment both the frequency  $\Delta\omega$  and the laser intensity  $I$ . Therefore, the correspondent  $\rho$  must depend on the intensity [ Fig. 4 ] or on the frequency [ Fig. 5]. The simplest calculation show that the saturation is at  $\Delta\omega \simeq 0,02 \Omega$  and absorption begin at  $\Delta\omega \simeq \Omega$ . As the  $\Gamma$  is return size of the time, it is possible to transfer a condition of saturation to language of the time-table interaction [32]. At the fixed frequency [ Fig. 4 ], when increase of intensity of the laser, the saturation comes at the maximal size of  $\Gamma$ , that corresponds to the minimal time. Very important the fact of weak growth is that means that the time too gradually decreases aspiring to a limit. On the other hand at a weak intensity the time is very large also grows indefinitely. At the fixed size of intensity of the laser [ Fig. 5], the condition of an exact resonance coincides with a condition when time is equally practically to zero and then it is gradually increased to indefinitely in process of a distance from a resonance [32]. If now to put in conformity a parity between frequency  $\Delta\omega$  of a field and  $k \cdot v$  where is the speed of atoms, becomes understandable that now it is possible to speak not only about time of interaction or time of life [32], but also about speeds of atoms, because it is supposed that is possible to replace one ( $\Delta\omega$ ) with another ( $k \cdot v$ ) accordingly. However, if we can put ( $\Delta\omega$ ) as a constant, another  $v$  is only one part of the distributions function.

When the condition for the near resonant condition is  $\Delta\omega \gg \gamma$  for the quantum interference condition of the EM field, then the rate  $R_2$  is simply [31]:

$$R_2 = \frac{\Gamma}{2} [1 - J_0(2\rho)], \quad (31)$$

where  $J_0$  is a Bessel function. Practically situation is as for one frequency, but with important features [ Fig. 6] due to a Bessel function.

With relation between  $k \cdot T$  and the rate  $R$  all figures becomes clearly observed due to connection of the temperature with the atomic velocity. Other atoms have conserved high velocities. Therefore the inelastic collisions should be expected. The general velocity distribution can be changed and the satellite distribution can be observed due to laser induced collisions between atoms.

## REFERENCES

- [1] C.J.Sansonetti and B.Richou, R.Engelman,Jr., L.J.Radziemski, *Phys. Rev. A*, **52**, 4, 2682 (1995 ).
- [2] N. V. Karlov, B. B. Krynetskii, O. M. Stel'makh. *Sov. J. Quant. Electron.*, **7**(10), 1305, (1977), (AIP 1978).
- [3] M. Yamashita, H. Kashiwagi. United States Patent 4,149,077 , Apr.10, (1979).
- [4] T.Arisawa, Y.Maruama, Y.Suzuki, and K.Shiba, *Appl.Phys. B*, **28**, 73-76 (1982).
- [5] T. Suzuki, N. Nomura, M. Okamoto and Y. Fujii. *Vacuum* **47**, No. 6-8, 671, (1996).
- [6] E.Kovarski, A. Esaulov, Laser induced Li-Ar plasma production, Proceedings of International Conf. LAWPP-98, Argentina, (1998).
- [7] D. Veza, G. J. Sansonetti. *Z. Phys. D - Atoms, Molecules and Clusters*, **22**, 463, (1992).
- [8] Mark E. Koch et al. *Phys. Rev. A*. **19**, 3, 1052, (1979); *Phys. Rev. Lett.* **42**, 16, (1979).
- [9] C-J. Lorenzen and K. Niemax. *J. Phys. B: At. Mol. Phys.* **15**, L 139, (1982).
- [10] C. Valda, D.Veza et al. *Z. Phys. D. - Atoms, Molecules and Clusters*, **22**, 591, (1992).
- [11] J.Brust, D.Veza et al. *Z. Phys. D.* **32**, 305, (1995).
- [12] S. Kita and N. Shimakura, *Phys. Rev. A*. **55**, 5, 3504, (1997).
- [13] G. Shimkaver et al. *Phys. Rev. A*. **48**, 2, 1409, (1993).
- [14] M.Zemansky, *Molecular Spectroscopy*, London, (1994).
- [15] E. E. Whiting, *J. Quant. Spectrosc. Radiat. Transfer*, **8**, 1379, (1968).
- [16] E.Kovarski, Single mode operation for laser excitation of lithium, Proceedings of SOCHIFI-98, Chile, (1998).
- [17] P.W.Smith, Proceedings of the IEEE,**60**, 4, 423 (1972).
- [18] S.Skowronek and A.Gonzalez Urena, *Rev.Sci.Instrum.*, **67**, 7, 2463 (1996).
- [19] M.Born and E.Wolf, *Principles of Optics*, ISBN 0-08-026482,Sixth Ed.,Pergamon Press (1980).
- [20] N. Shinohara, K. Okamoto. *Nuclear Instruments and Methods in Physics Research* **A362**, 114, (1995).
- [21] I.I.Sobelman, L.A.Vainshtein, E.A.Yukov, *Excitation of atoms and broadening of spectral lines*, Springer series on Atoms+Plasmas, Second Edition, ISBN 3-540-58686-5 (1995).
- [22] M.Marinescu, D.Dalgarno, *Phys.Rev.* **A52**, 311, (1995)
- [23] D. D. Konowalow, J. L. Fish. *Chemical Physics*, **77**, 435, (1983).
- [24] W. Demtröder. *Laser Spectroscopy*, Springer V., (1996).
- [25] D. D. Konowalow, J. L. Fish. *Chemical Physics*, **84**, 463, (1984).
- [26] W. R. Smyth. *Static and Dynamic Electricity*, New York, p. 251, (1950).
- [27] D. C. Thompson, B. P. Stoicheff. *Rev. Sci. Instruments*, **53**(6), 822, (1982).
- [28] Evgueni V. Kovarski, *Sov. J. Fizika Tverdogo Tela (Solid State Physics)*, **19**, 3, 905, (1977).
- [29] S. N. Atutov, B.V. Bondarev et al. *Optic Communications*, **115**, No. 3 - 4, p. 276, (1995).
- [30] Curtis C.Bradley and Randall G.Hulet, *Experimental methods in the physical sciences*, **29 b**, 129 (1996).
- [31] Evgueni V.Kovarski physics/0102018
- [32] Evgueni V.Kovarski quant-ph/0107079

## VI. FIGURE CAPTION

- Fig.1. Lithium 2S-2P absorption normalized spectrum with fitting  
Fig.2. Experimental setup for RIS of Lithium isotopes with Heat-Pipe oven and lasers.  
Fig.3. The electric current measurement.  
Fig.4 Saturation of the rate at the fixed frequency.  
Fig.5 The rate at the fixed intensity.  
Fig.6 The quantum interference rate at the fixed frequencies difference.

# Laser induced collisions between Lithium isotopes

Evgueni V. Kovarski  
*ekovars@netscape.net*  
(07.17.2001)

## Abstract

The near resonant cooling mechanism have offered for the experiment with laser induced excitation of Lithium isotopes and its ionization by collisions.

32.80.

Typeset using REVTeX



## I. INTRODUCTION

Clearly defined spectrum is the main requirement for any spectroscopical methods, which deal with two close isotopes as  $Li_6$  and  $Li_7$ , is preferable to use the atomic beams, where it is easy to realize the excitation of single spectral line of  $Li_6$  or  $Li_7$  [1]. However there are many publications devoted to the general study of Lithium vapor in the heat-pipe oven. There is the Doppler broadening of spectral lines. It is necessary to have a stability and accuracy frequency adjustments of the laser. Usually for Lithium atom the single mode laser operation is need with stability and tuning of the laser frequency better then 1  $GHz$  at the resonant frequency. The first known publication with Lithium resonance ionization spectroscopy (RIS) was in 1977 [2]. There were photo-ionization cross section going from the  $2P$  level and the demonstration of the ion current by varying the dye laser wavelength correspondent to  $2S - 2P$  transition. Therefore this was the first work about the possibility of Lithium laser isotope separation. Two years later the US patent for Lithium laser isotope separation was accepted in 1979 [3]. The resonance ionization spectroscopy (RIS) of Lithium use two lasers with different frequencies. It is depend on intensities of both lasers for resonance excitation at  $2S - 2P$  and for the ionization from  $2P$  [4] (1982). The mixture of two gases in heat pipe usually is present due to chemical activity of Lithium contacts with optical windows of the heat-pipe oven. The Ar gas usually is present. Therefore one can to compare ions production by RIS in the heat-pipe with another similar method for the  $Li - Ar$  contact ionization based on the ion cyclotron resonance (ICR) isotope separation [5]. It should be noted here that we shall not discuss the effectiveness methods of isotope separation, but on the other hand, both RIS and ICR can work more successfully at experiments where the concentration of Lithium atoms is high. To achieve high values of concentration it is necessary to increase the temperature of  $Li$  of a vapor chamber with the metallic Lithium. The ion generation process is important for some applications at similar condition of environment. We consider collisions at the experiment with heat-pipe oven, filled with  $Li - Ar$  mixture For such experiment the electromagnetic properties of gas mixture play an important role due to relatively high concentration of charged particles produced by emission, atomic collisions and proper RIS for ionization. The geometric distribution of generated positive and negative particles in the gas chamber is along the way of coaxial laser beams. If there is no voltage applied to electrodes the small value of electric current is only due to atom - field interaction. Because the heat pipe oven has two electrodes with cylindrical symmetry and proper laser is as new cylindrical electrode that produced charged particles along the laser way.

We are going to present: the simplified method for spectroscopic investigation of the dense vapor of  $Li - Ar$  mixture, based on methods of atomic collision estimations; the experimental setup for ionization experiment with lasers, precisely tuned on transition frequency; the results of electric current measurements. The ion generation is with both the RIS and without it. Last process is most interesting to that the ultra-violet radiation is absent and for achievement of a threshold of ionization is no sufficiently only to excite  $2S - 2P$  transition. In both cases the quantity of the charged particles can appear so large, that it is possible to speak about presence low density plasma [6]. The measurement of the excitation and ionization of dense lithium vapor by cw- dye laser with wavelength  $610.3nm$  were performed in Ref. [7]. In present work the result was obtained by using only  $670.8nm$  wavelength. When the DYE laser excite  $2P$ -level at  $1,848 eV$  it can not reach to  $3D$  energy

level at 3,879 eV due to 2,031 eV difference for two steps excitation and it can lower the ionization potential at 5,391 eV of *Li* atoms. For this reason we think that there is not a special two-step absorption process, so we will to discuss two mechanisms such as associative reaction and near resonance cooling.

## II. SPECTRAL CHARACTERISTICS OF THE DENSE LITHIUM VAPOR.

We begin with note that the main problem for such experiments is about the relative values for concentrations of neutral atoms and molecules in the same *Li* vapor. Of course, special measurements for molecules or clusters concentration are needed on time (for *Li* molecules studies see e.g. ref [8]). The standard experimental absorption intensity spectrum of the  $2S - 2P$  of each Lithium isotopes has two spectral lines *D1* and *D2* [1] with correspondence to level isotope shifts [9]. The Lithium  $2S - 2P$  has one doublet with distance of 10 GHz (0,012 nm) between *D1* and *D2* spectral lines. The isotope shift between *Li<sub>6</sub>D2* (670,7922 nm) and *Li<sub>7</sub>D2* (670,7764 nm) is 10,5333 GHz and between *Li<sub>6</sub>D1* (670,8073 nm) and *Li<sub>7</sub>D1* (670,7915 nm) is 10,5329 GHz [1].

Usually the observable at heat-pipe experiment  $2S - 2P$  spectrum of natural Lithium consists of three lines, where the central line is formed by the superposition of two lines going from two different isotopes [3]. At heat-pipe experiments with the dense *Li* vapor at high temperature, above 1000 K, all Gauss lines profiles can not been clearly observed. There are only three observable normalized profiles of absorption intensity received from experiment and fitted numerically. The well known picture of the fine structure for each isotope was not at high temperature heat pipe experiment, but particularly was revised with two diode laser for calibration.

The Voigt profile approach can be applied for simple analysis of the Doppler broadened line and for the Lorentzian line, which widths are related to the correspondent Gauss to Lorentz ( $G/L$ ) damping constant. With known value of the ( $G/L$ ) damping constant from fitted profile, it is easy to obtain the line width for Lorentzian profile and evaluate the summary of excitation transfer mechanisms. Also special experiments and theory are needed for detailed investigation of *Li* atoms collisions [10] - [13].

We use the method based on dense gas absorption intensity spectrum [Fig. 2] that can be analytically described by empirical approximation for a Voigt profile of the absorbed intensity in the Beer law, where the absorption coefficient  $k_{abs}$  is [14]:

$$k_{abs} = k_G \left[ e^\eta - \frac{2a}{\sqrt{\pi}} (1 - 2\eta F) \right], \quad (1)$$

The absorption coefficient for Gauss line profiles is  $k_G$ . The coefficient  $k_G$  can be founded numerically from fitted profiles of absorption intensity, because the application of the Beer law with absorption coefficient as a constant, which no depend on Gauss distribution is not correct for a dense vapor. Also at a maximum of one unsaturated line is possible to compare  $k_G$  form fitted spectrum with the same value from the Beer law, therefore is possible to use the thickness (8,5 cm) of dense vapor. There are two numerical parameters for normalized profile of intensity  $I_{abs}/I_0$ , where  $I_0$  is the intensity of the laser. One of these parameters is  $k_G$ , which depend on spectral lines saturation, e.g. for *Li<sub>6</sub>* and *Li<sub>7</sub>* due to accordingly

concentrations. The  $\eta$  is the second numerical parameter. It dependent on wings of spectral line at frequency  $\nu$ , which are far from the central line  $\nu_0$  for both isotopes:

$$\eta = \frac{(\nu - \nu_0)}{\Delta\nu_G} \sqrt{\ln 2}, \quad (2)$$

For unsaturated spectral lines, as for left spectral profile in the [ Fig. 1 ], that corresponds to  $Li_6$ , the parameter  $\eta$  leads to the function  $F$  for the Voight profile:

$$-2\eta F = 1 - 2\eta^2 + \frac{4}{3}\eta^2 - \frac{8}{15}\eta^6 + .. \quad (3)$$

and the  $(G/L) = a$  damping constant is

$$a = \frac{\Delta\nu_L}{\Delta\nu_G} \sqrt{\ln 2}. \quad (4)$$

The Eq. (3) is used only for the fitting  $Li_6$  spectral lines, because the parameter  $\eta$  for  $Li_6$  is not too large as for  $Li_7$ , due to the relative concentrations of these isotopes. For  $Li_7$  isotope spectral line the saturation is much more greater than for  $Li_6$ , thus in this case the Voight profile must be fitted by using the other sequence:

$$1 - 2\eta F = - \left( \frac{1}{2\eta^2} + \frac{3}{4\eta^2} + \frac{15}{8\eta^6} + \dots \right) \quad (5)$$

By fitting the experimental spectrum with above method is possible to obtain a better result with experiment for each spectral line. Also another empirical approximation of Voight profile [15] can be used successfully for all spectral lines at the narrow part of frequency spectrum.

The  $(G/L)$  damping constants for both  $Li_6$   $D_1$  and  $Li_7$   $D_2$  have the same values  $a_7 = a_6 = 0.021 \pm 0.0005$  and both absorption coefficients for  $Li_7$  and  $Li_6$  were estimated from fitted spectrum at a fixed temperature.

The relation of two Gaussian profiles for  $Li_7$  and  $Li_6$  at fixed temperature is:

$$\frac{\Delta\nu_{G6}}{\Delta\nu_{G7}} = \frac{\nu_{6D1}}{\nu_{7D2}} \sqrt{\frac{\mu_7}{\mu_6}} = 1,08, \quad (6)$$

where  $\mu_6 = 6,01703 a.u.$ ,  $\mu_7 = 7,01823 a.u.$  and resonance frequencies corresponds to wavelength 670,7764 nm for  $Li_7$  and 670,8073 nm for  $Li_6$ . At temperature  $T = 831.84K$  and pressure 1.8 torr, the full width of the half maximum (FWHM) is  $\Delta\nu_{G6} = 3763.17 MHz$  for  $Li_6$   $D_1$  and  $\Delta\nu_{G7} = 3484.58 MHz$  for  $Li_7$   $D_2$ .

For correspondent Lorentzian profiles one can easy to calculate the FWHM equal to  $\Delta\nu_{Li6} = 94.92 MHz$  for  $Li_6$   $D_1$  and  $\Delta\nu_{Li7} = 87.89 MHz$  for  $Li_7$   $D_2$ .

The heat velocity of atoms in the  $Li - Ar$  mixture is:

$$\bar{v} = \sqrt{\frac{8k_B T}{\pi M}} \quad (7)$$

Also the numerical equation for corresponded temperature dependence is  $\bar{v} = 63.64\sqrt{T}$ , where the reduction mass is  $M = (M_{Li}M_{Ar}/M_{Li} + M_{Ar}) = 0.8683 \cdot 10^{-26} kg$ .

Therefore, with the temperature about  $650\text{ K}$ , the random velocity of the  $Li - Ar$  atoms vapor is about  $160\ 000\text{ cm/s}$  and the correspondent Doppler shift for one laser wave is about  $16\text{ GHz}$ . There are some experimental possibilities for measurements. When the laser has frequency scanning along spectrum of Lithium, the relative datum can be used for the line position in the spectrum due to the Doppler shift for each wavelengths. The Doppler-free method, that used two opposite propagated beams with the same frequency on the each laser beam is free of the Doppler shift for detectors, thus the Lorentzian profile can be experimentally received, but only calibrated relative scale of the frequency can be used for estimation of the Lorentzian profile. Therefore the  $20\text{ GHz}$  scale between known spectral lines captured from the literature datum for  $Li$  is no good for Doppler-free experimental estimations of the Lorentzian profile in the gas chamber, because expected value of the FWHM is about  $100\text{ MHz}$  and special calibration laser air wavelength is needed. Also if the one of two laser beams is controlled by wave meter and another laser is controlled by a power meter or by photo diode with oscilloscope, thus the resolution of the wave meter is about  $0,0002\text{ nm}$  or  $133\text{ MHz}$  at  $670\text{ nm}$  and can not permit well accuracy for experiments with a Heat-pipe oven where all spectral lines are Doppler broadened and saturated. The  $2S - 2P$  transition of Lithium isotopes is well known for the all 4 principal spectral lines including the fine structures ( $fs$ ). Each atom has the lowest  $2S$  level with two ( $fs$ ) levels, which can be observed only at the special experiment with electric or magnetic fields. The distance between both  $fs$  levels is  $803\text{ MHz}$  for  $2S$  and  $18\text{ MHz}$  for  $2P$  level. Yet, we can put fine structures ( $fs$ ) out of our consideration the resonance  $2S - 2P$  transition with resonance frequency  $\omega_0 = 2,8 \cdot 10^{15}\text{ rad./s.}$ , because the Doppler - free method can not to permit the accuracy experiment with a given transition.

### III. EXPERIMENTAL SETUP

The selection and specification of special designed lasers instrumentation for selective excitation of lithium isotopes and full ionization is important because of the small frequency distance between the lithium lines is present and it is necessary to study some laser spectral stability characteristics. The experimental setup [ Fig. 2] consists of three lasers which path is the same route across the heat-pipe oven. This is possible by use properties of Glan prisms and rotators of polarization.

The lasers wavelength was controlled by a serial pulsed Burleigh wave meter Model WA 4500 with accuracy  $0,0001 - 0,0002\text{ nm}$  at wavelength range from  $1100\text{ nm}$  to  $400\text{ nm}$ . The laser line shape was measured by use of a Burleigh Spectrum Analyzer System SA 385 with SA-91 Etalon Assembly. Its maximum specified resolution is  $27\text{ MHz}$  using  $8\text{ GHz}$  FSR mirror set with finesse about 300 and the transmission more then 10 as a Fabry-Perot filter with thermal sensitivity  $70\text{ nm/}^\circ\text{C}$  changing in mirrors spacing.

The laser power was measured with a cw - Laser Power Meter, Spectra Physics, Mod 407 A. It has a wavelength range  $250 - 1100\text{ nm}$ , power range from  $5\text{ mW}$  to  $20\text{ W}$  with sensitivity variation about 1 because the damage peak energy density is  $0,3\text{ J/cm}^2$  at  $50\text{ ns}$  pulses. Also the 818 UV, Newport Power Meter was used for precisely measured power of low intensity cw - lasers.

For the ionization process we used a High Power  $Q$ -Switched,  $TEM_{00}$  frequency-doubled Nd-YAG *Lee* Laser, Model *815TQ*. The power stability was  $10\ 1064\text{ nm}$  was  $15\text{ W}$  at 5

$kHz$  repetition rate (pulse energy 2 ,2  $mJ$  and pulse duration 90  $ns$ ) and the intensity 3  $MW/cm^2$ . In this configuration the second harmonic wavelength (532  $nm$ ) is emitted laterally from the optical axis of the laser resonator. The SHG assembly contains a KTP (potassium titanyl phosphate crystal) which is bounced inside a temperature controlled chamber. Because of the small crystal cross section (4 x 4  $mm$ ), there is a little box for misalignment of the crystal with the Nd-YAG beam optical center line. The average power was 2,5  $W$ , the average energy was 0,5  $mJ$  and the pulse duration was 100  $ns$ . We worked with 1,5  $W$  for obtaining UV 266  $nm$ . For this purpose we used an *INRAD* temperature stabilized crystal of *KDP*, obtaining 40  $mW$  of the average power. The non-critical phase matching temperature (35  $^{\circ}C$  - 75  $^{\circ}C$ ) is quite dependent on the deuteration level of the *KDP*. Also the incoming edge of the crystal is at 90  $^{\circ}$  with the optical axis of the crystal and the reflection at the angle about 23  $^{\circ}$  decrease the intensity of 532  $nm$  about two times. The lineal polarization of 532  $nm$  going from the *LEE* laser had an inclination with the angle 45  $^{\circ}$  respect to the optical path of our experiment. The specially oriented crystal *KDP* for second harmonic generation (*SHG*) was needed. From two waves within one laser beam with  $\lambda = 532$   $nm$  the well known procedure of the second harmonic generation was used. The wave with  $\lambda = 266$   $nm$  We obtained a UV-beam at 266  $nm$  with intensity 16  $kW/cm^2$  after the prism separation from incoming 532  $nm$  wave. The line width of the UV line was 20  $MHz$  with high frequency stability. Frequency stability of the ionization laser is no so critical as for the excitation process, because for ionization we have a transition from  $2P$  to above ionization limit.

The group of calibration lasers consist both the 6202 *NewFocus* diode laser and the *EOSI* diode laser with line width about 100  $KHz$  and the average power 6  $mW$ . These lasers was used for calibrating the experiment due to high stability parameters at the needed wave length.

We tested a cw - broadband standing-wave Spectra Physics DYE Laser (Model 375 B), because we can change the mode structure of outgoing laser wave as a special background for given laser equipment [16]. The DYE laser was pumped by a power  $P_0 = 6W$ , Stability Multiline Ar-Ion Laser Spectra Physics Model 2017 -06 S. The Ar-ion laser had some measurable spectral lines, such as: at 514,5  $nm$  with 0,393  $P_0$ , at 496,5 $nm$  with 0,166  $P_0$ , at 488  $nm$  with 0,285  $P_0$ , at 476,5 $nm$  with 0,109  $P_0$ , at 457,9  $nm$  with 0,047 $P_0$ . The amplitude stability of the DYE laser intensity was best with pumping of the Ar-Ion laser at 514,5  $nm$ . The DYE laser was based on DCM 4 -(Dicyanomethylene) - 2 -(methyl) - 6 -(p - dimethylaminostyryl)- 4-H-(pyran) with molecular weight 303,37  $a.u.$  and concentration 1,5 ( $mmole/l$ ), which was prepared when 0 ,682g of the DCM was solved in Propylene carbonate (0 ,6  $l$ ) and Ethylene Glycol (0,9  $l$ ). The absorption curve of DCM has an absorbency region between 450  $nm$  and 550  $nm$ . The broad band emission curve has the FWHM about 80  $nm$  at 650  $nm$ , which is close to the resonance  $2S - 2P$  transition of Lithium at 671  $nm$ . The Spectra Physics data for the Model 375 B laser were: power 600  $mW$  at 705  $nm$ , line width 7  $GHz$ , amplitude stability less then 0 ,5 accuracy of wavelength changing 0 ,5  $nm$ . The limit of wavelength changing is in the same order as a Rayleigh selection rule for spectral lines  $8/\pi^2$ , that is about 0,5  $nm$  for a given laser line width. We obtained characteristics of Spectra Physics DYE laser, Model 375 B, such as: average power 1 ,2  $W$  at 671  $nm$ , accuracy of changing wavelength better then 0,01  $nm$  and frequency stability about 0,0001  $nm/hour$  during time of the experiment. All parame-

ters are depended on needed laser modes structure and corresponds to properties of optical elements inside the resonator. For our experiments with  $Li$  we modified the mode structure and the spectral line width of outgoing laser wave by inserting an additional etalon into a laser resonator. We note that broadband laser had the tuning accuracy  $0,5 \text{ nm}$  without  $E1$  due to  $BF$  frequency tuning accuracy. With  $BF$  and  $E1$  the frequency tuning accuracy was measured  $\approx 0,0001 \text{ nm}$ . The first air spaced etalon ( $E1$ ) had a temperature stability. When the  $BF$  and  $E1$  were used, the output frequency of the DYE laser was tuned to the quite frequency  $4,46789597 \cdot 10^{14} \text{ Hz}$  by used the angle and temperature tuning of  $E1$ . The FSR of output frequency was  $19,655 \text{ GHz}$ . Then the second etalon  $E2$ , with  $\text{FSR} = 15 \text{ GHz}$  was installed inside the cavity and the same operation was repeated with angle tuning of  $E2$  for the same frequency. The  $E2$  was chosen, because the spectral lines of the Lithium have  $10 \text{ Ghz}$  distance twice between 3 spectral lines and laser with  $BF$  and  $E1$  can excite both  $Li_6$  and  $Li_7$ . The single mode operation of the broad band laser was achieved. The single mode selection was realized experimentally [Fig. 2] by use the aperture with diameter  $1 \text{ mm}$  for transverse mode selection and, by use two etalons ( $E1, E2$ ) and the birefringent filter ( $BF$ ) for longitudinal mode selection. The mode structure of the single laser beam is very important for selective excitation. There are some experimental possibilities with the broad band DYE laser, which depend on needed experiments. The single mode operation was necessary for a RIS experiments. On the contrary for measured values of electric current [Fig.3] of the laser induced low density plasma observation experiment [6], the DYE laser had the two longitudinal modes with FWHM  $100 \text{ MHz}$ , separated exactly at  $20 \text{ GHz}$  with cavity etalon. This etalon had the free spectral range (FSR) that correspondent the distance between two spectral lines of  $Li_6$  and  $Li_7$  isotopes of the natural Lithium vapor. The laser was tuned exactly on  $670.8073 \text{ nm}$  for  $Li_6$ . Another wavelength  $670.7716 \text{ nm}$  was not controlled. The average power at this experiment was  $100 \text{ mW}$ . There are some known methods of longitudinal mode selection by use interferometers techniques as in [17], [18]. The free spectral range FSR is equal to the distance between two longitudinal modes:

$$FSR_\nu = \frac{c}{2\eta_t d \cos \Theta_i} \quad (8)$$

Thus, with variation of the angle, some longitudinal modes of the laser will have not losses for correspondent frequencies  $\nu = m$ , (FSR), and it is possible to move the Airy spectrum of the etalon along the frequency axis up or down to quite position. The longitudinal modes are spaced in frequency by  $c/2L$ . We note that for near-confocal resonator the free spectral range (FSR) is:

$$\delta\nu = \frac{c}{4L + \frac{x}{\rho^3}}, \quad (9)$$

where ( $x$ ) - is the distance from the axis and  $\rho$  is the radius of mirrors, when  $L = \rho$ . Thus the series of longitudinal modes are separated by  $c/4L \approx 250 \text{ MHz}$  for a cavity with  $L \approx 30 \text{ cm}$ . Transverse modes are important for a mode selection too. Amplitude distribution of these modes is given with Hermit polynomial  $TEM_{mn}$  modes. The separation of the first transverse mode ( $m = 0, n = 1$ ) from the axial mode is:

$$\frac{\nu_1 - \nu_0}{\nu_0} = 2,405 \frac{\lambda^2}{8\pi^2 r^2}, \quad (10)$$

where ( $r$ ) is diameter of cylindrical laser material. In deriving the Van Cittert-Zernike theorem [19] it follows that the diffraction pattern would be obtained on replacing the source (the DYE luminescence cross section) by a diffraction aperture of the same size and shape as the source. The amplitude distribution over the wave front in the aperture being proportional to the intensity distribution across the source. The calculation of the complex degree of coherence of light from an incoherent source, by use the Hopkins formula [19], leads to the mirrors diameter  $0,32 \lambda f/h$ , where ( $f$ )- is focal distances,  $h \approx 10 \mu m$  - is the diameter of the source, that dependent on a pumping of the focused laser (6 W Ar-Ion laser) and thermal lens. At flow velocities of the DYE about 10 m/s the time of flight for the dye molecules through the focus is about 1  $\mu s$ . By using a mirror whose reflectivity can be varied over its surface, it is possible to have some given combination of transverse modes, if it is necessary.

There are two problems of frequency stability of the DYE laser. Firstly, we note that the material of installed cavity DYE laser etalon was fused silica. Regardless of thickness it has a drift of airspace between fused silica plates about 5 GHz/ $^{\circ}C$  and would have to be temperature stable about 0,1  $^{\circ}C/hour$ . Secondly, the environment conditions are very important for stable laser experiment with atomic spectral lines. Therefore, there is the frequency drift:

$$\frac{\Delta\nu}{\nu} = \frac{\Delta d}{d} + \frac{\Delta n}{n} \quad (11)$$

where ( $d$ ) is the cavity length and ( $n$ ) is the refraction coefficient. For the quartz rod resonator structure of the DYE laser, Model 375D, we have with respect to the change of a cavity length a resulting temperature sensitivity about 90 MHz/ $^{\circ}C$ . With respect to the refraction coefficient of air we found a temperature sensitivity about 410 MHz/ $^{\circ}C$ . The amplitude and frequency stability of the laser was maintained during 3 hours of the experiment. The wavelength control had the accuracy 0.0001 nm by use the serial wave meter. The measured value of the line width was about 100 MHz for cw -regime of DYE excitation by use the focused Ar - Ion laser. Another excitation of the same DYE laser was with 120 ns pulses of twice doubled Nd:YAG laser at 266 nm, with 5 KHz pulse repetition and average power about 1 W. Output pulses from the DYE laser were 100 ns.

#### IV. EXPERIMENTAL RESULT

For a known value of the ( $G/L$ ) damping constant and absorption coefficient from described method of the fitting we can exam the concentration of the both isotopes:

$$N_{6G} = k_{6G} \left[ \frac{2\sqrt{\pi}}{\lambda_{6D1}^2} \right] \frac{1}{a}, \quad (12)$$

$$N_{7G} = k_{7G} \left[ \frac{\sqrt{\pi}}{\lambda_{7D2}^2} \right] \frac{1}{a}, \quad (13)$$

where the absorption coefficients given from fitted profiles are  $k = 0.6 \text{ cm}^{-1}$  for  $Li_6$  and  $k = 14.75 \text{ cm}^{-1}$  for  $Li_7$ . The correspondent concentration going from above formulas is

equal to  $2.25 \cdot 10^{10} \text{ cm}^{-3}$  for  $Li_6$  and  $27.65 \cdot 10^{10} \text{ cm}^{-3}$  for  $Li_7$ . So the relation of two concentrations is  $N_6/N_7 = 0.08135$ , which is in well agreement with the characteristics of natural Lithium [20].

On the other hand, one can to verify values of Lithium concentration by use the following well known formula for the Lithium vapor pressure (in *torr*) at fixed temperature (in *K*):

$$P = 10^{5,055 - \frac{8023}{T}}, \quad (14)$$

where the vapor pressure for given temperature is equal to  $0.003427 \text{ Pa} = 0.0000257 \text{ torr}$ . By using the equation of the state for ideal gas  $P = Nk_B T$  and Eq.(10), one can obtain the concentration of the natural Lithium, which is equal to  $29.85 \cdot 10^{10} \text{ cm}^{-3}$ . The Heat-pipe was filled with *Ar* gas with the concentration  $10^{17} \text{ cm}^{-3}$ .

When resonance excitation of the considered system  $Li(2^2S) - (2^2P)$  was realized by  $671 \text{ nm}$  cw-laser, the ionization process was registered. The result of ionization by  $671 \text{ nm}$  was compared with additional UV laser for ionization from  $2S - 2P$  energy level ( $1,848 \text{ eV}$ ) to energy level of ionization limit ( $5,391 \text{ eV}$ ).

Intensity values of both the cw-DYE laser and the pulsed UV laser were changed correspondingly to the beam diameter  $3 \text{ mm}$  across the heat-pipe oven. We did not worked with specially applied to the heat-pipe electrodes voltage or load resistors.

Direct measurements of the electric current were performed by amper meter; maximum average value of the electric current was registered about  $30 \mu A$  [ Fig. 3 ]. We denoted three curves, where three principal effects were registered such as: (a) is the upper dependence for the RIS by use excitation and ionization from two lasers  $671 \text{ nm}$  and  $266 \text{ nm}$ . The RIS is more effective between  $450^\circ C$  and  $650^\circ C$ . (b) is the ionization current due to only  $2S-2P$  excitation with  $671 \text{ nm}$ . This specific ionization is more effective for highest temperatures. (c) is the lowest dependence (the noise) for a emission. Only small difference between average value of electric current due to the RIS process [ Fig. 3 -(a) ] and to resonance excitation  $2S - 2P$  [ Fig. 3 -(b) ]. The noise or the emission in temperature range from  $450^\circ C$  up to  $700^\circ C$  with electric current up to  $3 \mu A$  and capacitance up to  $20 \text{ nF}$  with observable saturation [ Fig. 3 -(c) ]. Values of the electric current varies from  $5 \mu A$  up to  $30 \mu A$  [ Fig. 3 -(a) ], and capacitance from  $10 \text{ nF}$  up to  $100 \text{ nF}$ . Also the capacitance of cylindrical heat-pipe was measured. The results of the current and capacitance measurements at the temperature higher than  $650^\circ C$  are the same for both mechanisms. Also it is easy to separate RIS from another ionization using the modulation signal measurements because RIS use the pulse UV laser.

## V. SOME MECHANISMS OF COLLISIONS

If the colliding particles have no charge, the trajectory  $r(t)$  is assumed to be rectilinear:  $r(t) = \rho + vt$ , where  $\rho$  and  $v$  are the impact parameter and relative velocity. The elastic collisions change the phase of damped oscillator,  $\phi(t)$ , but not the amplitude,  $x(t)$ , due to the frequency shift  $\Delta\omega$  during the phase-perturbing collisions. If the duration of collision,  $\tau_c$ , is short compared with the mean time between two consecutive collisions, one can neglect the radiation during collisions and consider the collisions to be instantaneous. Therefore the collisions are manifested only in phase shifts (Impact broadening approximation), where the



dimension parameter  $h = \rho^3 N_{Ar} \ll 1$  determines the number of perturbers in the Weisskopf sphere with the radius  $\rho$ , where the binary approximation holds. Depending on the type and states of interacting atoms both attraction and repulsion can take place at long distances. At short distances the potential is repulsive. In general case the interaction force is depends not only on spatial but also on angular variables. The results of calculations in which a more realistic interaction  $r^{-6}$  is used can not be described by a simple Lorentzian distribution, that depends on the type of the transition. The repulsive part of the interaction is usually taken into account in the form of Lennard-Jones potential. In general case, when the mean distance between the atoms is of the same order with the magnitude of atomic dimensions, simple expression for potential  $V(r) = C_6/r^6$  is valid with approximations due to both instantaneous dipole-dipole interaction and dipole-quadruple interaction with  $C_8/r^8$ .

The shift,  $\Delta\omega = 2\pi\Delta\nu$ , and broadening,  $\Gamma$ , of the Lorentz spectral distribution [21] are:

$$\Delta\nu = 2.91C_6^{\frac{2}{5}}v^{\frac{3}{5}}N_{Ar} , \quad (15)$$

$$\Gamma = 2\pi\Delta\nu_L = 8.16C_6^{\frac{2}{5}}v^{\frac{3}{5}}N_{Ar} , \quad (16)$$

For a temperature  $T = 831K$ , which we used for a fitting procedure, one can easily obtain the value for a FWHM of the Lorentzian profile,  $\Gamma = 617rad \cdot s^{-1}$  or  $\Delta\nu = 98.2MHz$  by using the coefficient in the length form  $C_6=1406$  a.u. [22] for  $Li(2^2S) - (2^2P)$ , where two interacted atoms, one of which  $2^2P$ , are in different angular momentum states with associated magnetic quantum numbers  $M_2 = \pm 1$  and attractive or repulsive interaction are. Also for  $Li(2^2S) - Li(2^2S)$  the value of  $C_6=1390$  a.u.  $= 1390 e^2a_0^2 = 1.330786 \cdot 10^{-76} Cl \cdot V \cdot m^6$  [23] is closely to estimation of  $C_6$  for  $Li(2^2S) - (2^2P)$  interaction. For this reason the measured ionization gives the answer about the nature of interaction in favor of  $Li(2^2S) - (2^2P)$ .

Therefore the value of  $\Delta\nu = 98.2MHz$  which can be obtained by use  $C_6$  coefficient well corresponded to experimental results  $\Delta\nu_{L6} = 94.92MHz$  for  $Li_6 D_1$  and  $\Delta\nu_{L7} = 87.89MHz$  for  $Li_7 D_2$  from the fitting procedure.

The shift of the spectral maximum position measured at two temperature points are  $0.0126MHz/K$  or  $1.26MHz/torr$ . The value of the FWHM temperature deviation is  $0.0353MHz/K$  due to the principal temperature dependence  $\Delta\nu \simeq T^{0.3}$ , which implies the correspondent pressure changing as  $3.53MHz/torr$  (for a comparison see results for  $Li$  in ref. [24]).

The impact parameter or Weisskopf radius is [21]:

$$\rho = \left( \frac{3\pi C_6}{8v} \right)^{0.2} \quad (17)$$

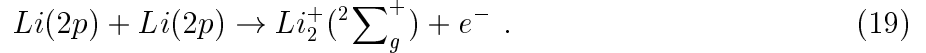
For a temperature range from  $500^\circ C$  to  $750^\circ C$  the impact parameter varies from  $6.685\text{\AA} = 12.63a_0$  to  $6.5\text{\AA} = 12.28a_0$ . The cross section is  $\sigma \simeq \pi\rho^2 = 132.7\text{\AA}^2 = 1.33 \cdot 10^{-14} cm^2$ .

The minimum concentration of charged particles in  $Li - Ar$  mixture at temperature  $1000 K$  can be estimated by taking into account the value of total current between two electrodes of Heat pipe as  $n_e \approx 10^6 cm^{-3}$ . Well-known Saha equation for amount of ionization  $n_e/n$  to be expected in a gas in thermal equilibrium

$$\frac{n_e}{n} \approx 2.4 \times 10^{15} \frac{T^{3/2}}{n_e} e^{-U_i/kT} \quad (18)$$

gives the ionization degree  $\approx 10^{-10}$  for *Li* (which concentration is  $n_{Li} \approx 10^{13} \text{ cm}^{-3}$  and ionization energy  $U_i = 5.4 \text{ eV}$ ) and  $10^{-36}$  for *Ar*, ( $n_{Ar} \approx 10^{17} \text{ cm}^{-3}$ ,  $U_i = 15 \text{ eV}$ ). So, the inelastic collisions between unexcited *Ar* and *Li* atoms could not provide the observed concentration of charge particles.

Such value of electron gas density, when DYE laser is applied [ Fig. 3 -(b) ], can be achieved due to the yield of the associative ionization reaction:



Such a process would be possible if the excited lithium atoms approached each other with relative kinetic energy about of  $0.46 \text{ eV}$  [25].

The simple approximation (18) shows that above associative ionization reaction can provide the electron densities up to  $n_e \approx 10^8 \text{ cm}^{-3}$  without the action of UV laser [ Fig. 3 -(b) ]. As for the rather high current observed even in the case when both lasers (DYE and UV) are shut down [Fig. 3 - (c)], such value of electron gas density can be achieved due to the effects of emission, mainly from the internal hot electrode with a mesh plating by Lithium.

The space-charge average current in Heat-pipe can be estimated by using the Child equation [26], due to the presence of cylindrical symmetry:

$$-I = \frac{8\pi\epsilon}{9} \sqrt{\frac{2e}{m_e}} \frac{V^{3/2}}{a\beta^2} , \quad (20)$$

where the parameter ( $\beta$ ) was determined in the Ref. [26] and ( $a$ ) is the radius of the external cylinder. The mean values for current and dielectric constant can be taken directly from current and capacitance measurements.

Given the natural line width equal to  $5,8 \text{ MHz}$  for the  $2P$  - energy level we obtain the absorption cross section

$$\sigma_{2s-2p} = 0,054 A_{2p-2s} \frac{\lambda^2}{\Delta\nu_D} \quad (21)$$

where  $A_{2p-2s} = 1/t_s$ , with  $t_s = 27,1 \text{ ns}$ . The Doppler line width of the *Li* was  $\Delta\nu_D = 2,5 \text{ GHz}$ . The absorption coefficient was  $0,154 \text{ cm}^{-1}$  in our Heat-Pipe experiment. For a given  $2S - 2P$  resonance excitation we measured absorption cross section

$$\sigma_a = 1,4 \cdot 10^{-12} \text{ cm}^2 \quad (22)$$

and ionization cross section for  $266 \text{ nm}$  ionizer:

$$\sigma_i = 1,2 \cdot 10^{-17} \text{ cm}^2 \quad (23)$$

The cathode emission current and the current of positively charged ions were also discussed in the Ref. [27].

The one-dimensional systems of driven charges can change symmetry in the phase pulses space, when the classical phenomena in one direction take into account quantization in others. It results in thermal drag effects in solids wires [28], but can result in thermal optical experiments too. Another effect is light-induced diffusive pulling (pushing) of lithium atoms into a laser beam, which was studied in Ar noble gas, where the value of diffusion coefficient  $4.3 \text{ cm}^2/\text{s}$  was measured [29].

It should be noted here, that the peak concentration of charged particles produced by the RIS [ Fig. 3 -(a) ] using  $77 \text{ ns}$  UV pulses is much more higher than the measured average value.

An estimation, given even for the minimum value of  $n_e \approx 10^6 \text{ cm}^{-3}$ , gives the value of Debye length  $\lambda_D \sim 0.1 \text{ cm}$ , the number of charged particles inside the Debye sphere  $N_d \sim 10^5$  and  $\omega_p \nu_{ei} \sim 10^4$ , where  $\omega_p$  is the plasma frequency and  $\nu_{ei}$  is the collisions rate. It means that the *Li - Ar* mixture at temperature in the order of  $10^3 \text{ K}$  behaves like a plasma rather than a neutral gas [6].

By other hand we can discuss another mechanism for observed ionization . We will take the Doppler cooling as the one step to achieve the low temperature for the Bose-Einstein Condensate (BEC) at very low temperature. The limit of the temperature achieved for Lithium is  $140 \mu\text{K}$  by balance with a scattering force in a random direction [30]. The Doppler limit of achievable temperature ( $T$ ) is:

$$k_B \cdot T = \frac{\hbar \Gamma}{2} \quad (24)$$

where  $\Gamma$  is a damping constant.

Let's change this relation:

$$k_B T = \hbar \cdot \frac{R}{R_0} = \hbar \cdot R_1 \quad (25)$$

where the rate of the power absorption  $R_1$  for two level atomic system interacted with EM field is well known:

$$R_1 = \frac{2\Omega^2 \Gamma}{\Delta\omega^2 + 4\Omega^2 + \Gamma^2} \quad (26)$$

The Rabi frequency  $\Omega_\nu$  measured in ( $\text{MHz}$ ) is:

$$\Omega_\nu = \frac{d_{1,2} \cdot E_0}{\hbar} \quad (27)$$

with  $d_{1,2}$  - as the matrix dipole momentum and  $E$  as the amplitude of EM wave. There is the frequency  $\Omega$ , that make a round oscillations between two levels. When  $\Delta\omega \neq 0$ , one can used for a given *Li* atom the fixed value of the Rabi frequency  $1000 \text{ MHz.rad.}$ . Some inequalities are for given values in the denominator of the profile. One of this inequalities is evidently for an application, because the value of the Rabi frequency  $\Omega = \Omega_c = 1000 \text{ MHz.rad.}$  and  $\Gamma = 37 \text{ MHz.rad.}$  with  $\Omega \gg \Gamma$  :

$$R_1 = \pi \Omega_c \Gamma \left[ \frac{1}{2\pi} \frac{4\Omega_c}{(\omega - \omega_0)^2 + (2\Omega_c)^2} \right] \quad (28)$$

The rate  $R_1$  can be represented by use the parameter  $\rho$  that depend on the Rabi frequency and the frequency tuning value:

$$\rho = \frac{\Omega}{\Delta\omega} = \text{const} \left[ \frac{\sqrt{I}}{\Delta\omega} \right] \quad (29)$$

$$R_1 = \frac{\Gamma}{2} \left[ \frac{(2\rho)^2}{1 + (2\rho)^2} \right] \quad (30)$$

The well known saturation effect by intensity of the laser is clearly observed. Is possible to fix at experiment both the frequency  $\Delta\omega$  and the laser intensity  $I$ . Therefore, the correspondent  $\rho$  must depend on the intensity [ Fig. 4 ] or on the frequency [ Fig. 5]. The simplest calculation show that the saturation is at  $\Delta\omega \simeq 0,02 \Omega$  and absorption begin at  $\Delta\omega \simeq \Omega$ . As the  $\Gamma$  is return size of the time, it is possible to transfer a condition of saturation to language of the time-table interaction [32]. At the fixed frequency [ Fig. 4 ], when increase of intensity of the laser, the saturation comes at the maximal size of  $\Gamma$ , that corresponds to the minimal time. Very important the fact of weak growth is that means that the time too gradually decreases aspiring to a limit. On the other hand at a weak intensity the time is very large also grows indefinitely. At the fixed size of intensity of the laser [ Fig. 5], the condition of an exact resonance coincides with a condition when time is equally practically to zero and then it is gradually increased to indefinitely in process of a distance from a resonance [32]. If now to put in conformity a parity between frequency  $\Delta\omega$  of a field and  $k \cdot v$  where is the speed of atoms, becomes understandable that now it is possible to speak not only about time of interaction or time of life [32], but also about speeds of atoms, because it is supposed that is possible to replace one ( $\Delta\omega$ ) with another ( $k \cdot v$ ) accordingly. However, if we can put ( $\Delta\omega$ ) as a constant, another  $v$  is only one part of the distributions function.

When the condition for the near resonant condition is  $\Delta\omega \gg \gamma$  for the quantum interference condition of the EM field, then the rate  $R_2$  is simply [31]:

$$R_2 = \frac{\Gamma}{2} [1 - J_0(2\rho)], \quad (31)$$

where  $J_0$  is a Bessel function. Practically situation is as for one frequency, but with important features [ Fig. 6] due to a Bessel function.

With relation between  $k \cdot T$  and the rate  $R$  all figures becomes clearly observed due to connection of the temperature with the atomic velocity. Other atoms have conserved high velocities. Therefore the inelastic collisions should be expected. The general velocity distribution can be changed and the satellite distribution can be observed due to laser induced collisions between atoms.

## REFERENCES

- [1] C.J.Sansonetti and B.Richou, R.Engelman,Jr., L.J.Radziemski, *Phys. Rev. A*, **52**, 4, 2682 (1995 ).
- [2] N. V. Karlov, B. B. Krynetskii, O. M. Stel'makh. Sov. J. Quant. Electron., **7**(10), 1305, (1977), (AIP 1978).
- [3] M. Yamashita, H. Kashiwagi. United States Patent 4,149,077 , Apr.10, (1979).
- [4] T.Arisawa, Y.Maruama, Y.Suzuki, and K.Shiba, Appl.Phys. B.28, 73-76 (1982).
- [5] T. Suzuki, N. Nomura, M. Okamoto and Y. Fujii. Vacuum **47**, No. 6-8, 671, (1996).
- [6] E.Kovarski, A. Esaulov, Laser induced Li-Ar plasma production, Proceedings of International Conf. LAWPP-98, Argentina, (1998).
- [7] D. Veza, G. J. Sansonetti. Z. Phys. D - Atoms, Molecules and Clusters, **22**, 463, (1992).
- [8] Mark E. Koch et al. Phys. Rev. A. **19**, 3, 1052, (1979); Phys. Rev. Lett. **42**, 16, (1979).
- [9] C-J. Lorenzen and K. Niemax. J. Phys. B: At. Mol. Phys. **15**, L 139, (1982).
- [10] C. Valda, D.Veza et al. Z. Phys. D. - Atoms, Molecules and Clusters, **22**, 591, (1992).
- [11] J.Brust, D.Veza et al. Z. Phys. D. **32**, 305, (1995).
- [12] S. Kita and N. Shimakura, Phys. Rev. A. **55**, 5, 3504, (1997).
- [13] G. Shimkaver et al. Phys. Rev. A. **48**, 2, 1409, (1993).
- [14] M.Zemansky, Molecular Spectroscopy, London, (1994).
- [15] E. E. Whiting, J. Quant. Spectrosc. Radiat. Transfer, **8**, 1379, (1968).
- [16] E.Kovarski, Single mode operation for laser excitation of lithium, Proceedings of SOCHIFI-98, Chile, (1998).
- [17] P.W.Smith, Proceedings of the IEEE,**60**, 4, 423 (1972).
- [18] S.Skowronek and A.Gonzalez Urena, Rev.Sci.Instrum., **67**, 7, 2463 (1996).
- [19] M.Born and E.Wolf, *Principles of Optics*, ISBN 0-08-026482,Sixth Ed.,Pergamon Press (1980).
- [20] N. Shinohara, K. Okamoto. Nuclear Instruments and Methods in Physics Research **A362**, 114, (1995).
- [21] I.I.Sobelman, L.A.Vainshtein, E.A.Yukov, *Excitation of atoms and broadening of spectral lines*, Springer series on Atoms+Plasmas, Second Edition, ISBN 3-540-58686-5 (1995).
- [22] M.Marinescu, D.Dalgarno, Phys.Rev. **A52**, 311, (1995)
- [23] D. D. Konowalow, J. L. Fish. Chemical Physics, **77**, 435, (1983).
- [24] W. Demtröder. Laser Spectroscopy, Springer V., (1996).
- [25] D. D. Konowalow, J. L. Fish. Chemical Physics, **84**, 463, (1984).
- [26] W. R. Smyth. Static and Dynamic Electricity, New York, p. 251, (1950).
- [27] D. C. Thompson, B. P. Stoicheff. Rev. Sci. Instruments, **53**(6), 822, (1982).
- [28] Evgueni V. Kovarski, Sov. J. Fizika Tverdogo Tela (Solid State Physics), **19**, 3, 905, (1977).
- [29] S. N. Atutov, B.V. Bondarev et al. Optic Communications, **115**, No. 3 - 4, p. 276, (1995).
- [30] Curtis C.Bradley and Randall G.Hulet, *Experimental methods in the physical sciences*, **29 b**, 129 (1996).
- [31] Evgueni V.Kovarski physics/0102018
- [32] Evgueni V.Kovarski quant-ph/0107079

## VI. FIGURE CAPTION

Fig.1. Lithium 2S-2P absorption normalized spectrum with fitting

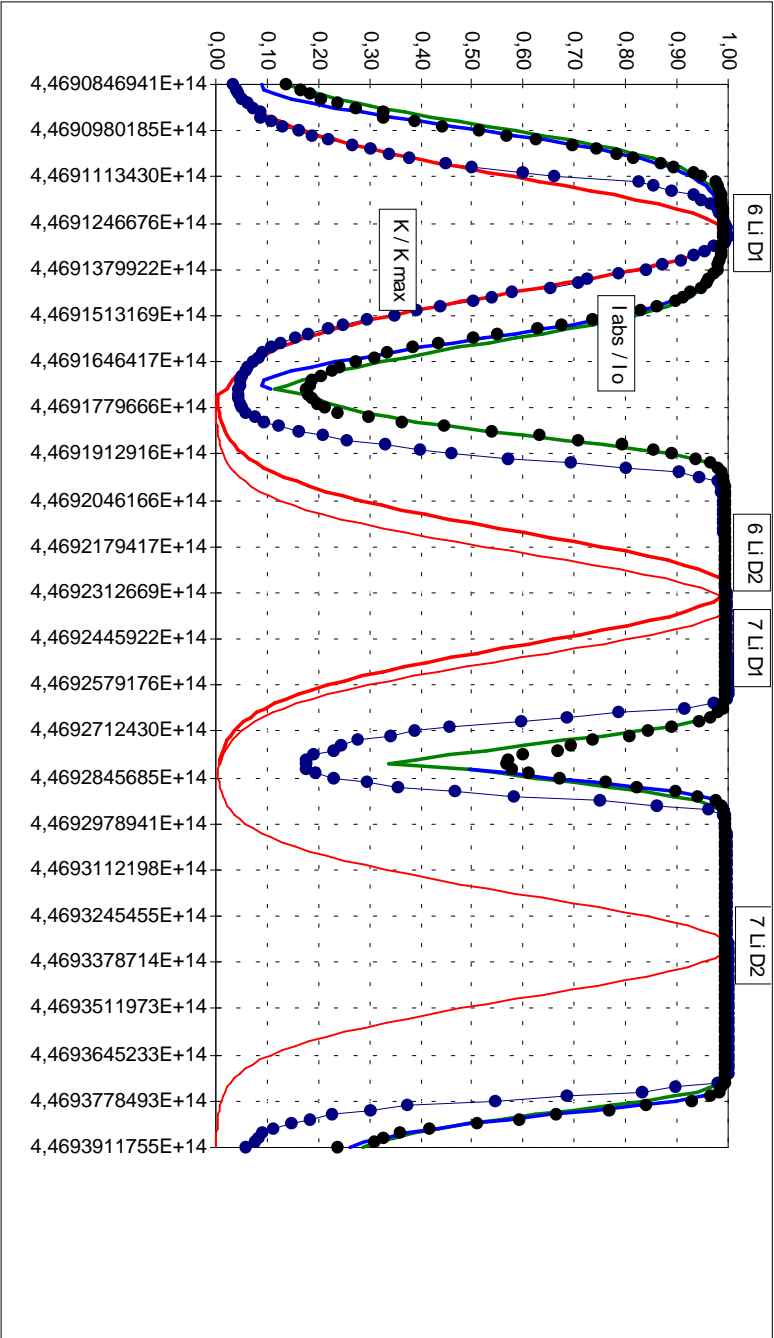
Fig.2. Experimental setup for RIS of Lithium isotopes with Heat-Pipe oven and lasers.

Fig.3. The electric current measurement.

Fig.4 Saturation of the rate at the fixed frequency.

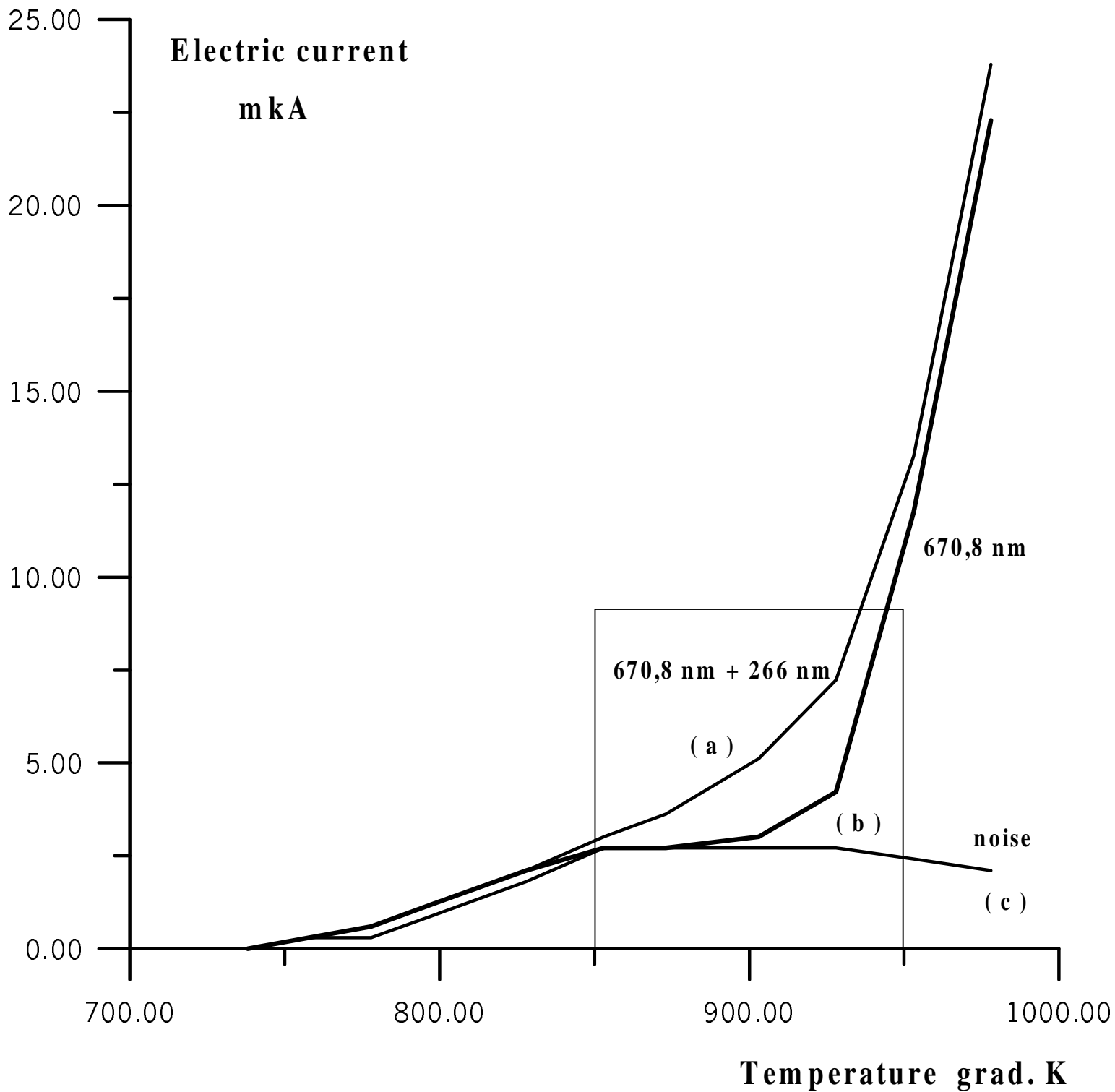
Fig.5 The rate at the fixed intensity.

Fig.6 The quantum interference rate at the fixed frequencies difference.



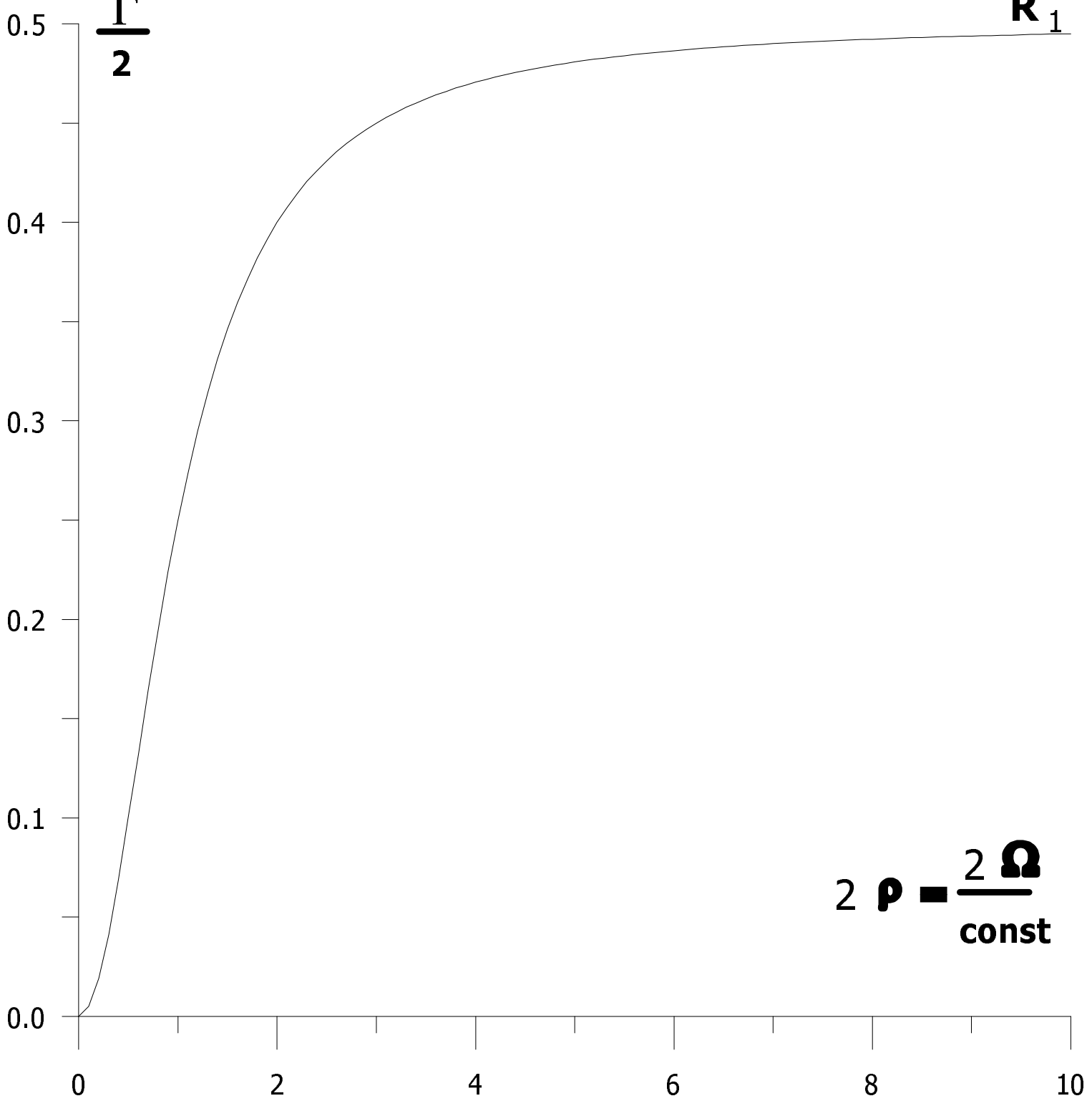






$$\frac{\Gamma}{2}$$

$R_1$



$$2 \rho = \frac{2 \Omega}{\text{const}}$$

